

Ice-Sheet Dynamics

Christian Schoof¹ and Ian Hewitt²

¹Department of Earth and Ocean Sciences, University of British Columbia, V6T 1Z4 Vancouver, Canada; email: cschoof@eos.ubc.ca

²Department of Mathematics, University of British Columbia, V6T 1Z2 Vancouver, Canada

Annu. Rev. Fluid Mech. 2013. 45:217–39

First published online as a Review in Advance on September 27, 2012

The *Annual Review of Fluid Mechanics* is online at fluid.annualreviews.org

This article's doi:
10.1146/annurev-fluid-011212-140632

Copyright © 2013 by Annual Reviews.
All rights reserved

Keywords

thin-film flows, thermoviscous feedbacks, free boundaries

Abstract

We describe the development of mathematical models of ice sheets, focusing on underlying physics and the minimal components that successful models must contain. Our review describes the basic fluid dynamical ice-flow models currently in use; points out numerous poorly understood thermo-mechanical feedbacks in ice flow; and describes the current, often poorly constrained, state of models for ice-sheet sliding and subglacial drainage, as well as their role in ice-stream dynamics. We conclude with a survey of marine ice-sheet models, outlining recent developments of self-consistent free-boundary models and ongoing research into three-dimensional marine ice sheets.

1. INTRODUCTION

Ice sheets form an integral part of Earth's climate system (Solomon et al. 2007). Their potential to alter sea levels is widely recognized (van den Broeke et al. 2011), but ice sheet–climate interactions also include effects on atmospheric circulation patterns (Roe & Lindzen 2001) as well as ocean overturning (Hemming 2004). Recent concern has been generated by dramatic examples of mass loss from the ice sheets in Greenland (Rignot & Kanagaratnam 2006) and Antarctica (Scambos et al. 2004). Although this concern is driven primarily by the specter of rising global surface temperatures, many of the observed mass-loss processes are not driven directly by ice surface melting. Instead, they involve the flow of ice, and this is the primary focus of our review.

We aim to give an account of mathematical models for a number of phenomena fundamental to the observed dynamics of ice sheets. This account is necessarily our own selective view of the subject: Studies of ice-sheet dynamics have grown enormously in scope recently, and a single, comprehensive overview is no longer feasible. Our main focus is primarily on ice-sheet physics. Rather than concentrating on numerical simulations of ice sheets in the context of climate change, we simply hope that our review pinpoints some avenues for improvement in the underlying mathematical models. Another recent review is Blatter et al. (2011), and a substantial book chapter in Fowler (2011) is devoted to ice dynamics. Cuffey & Paterson (2010) provide a comprehensive textbook that covers a much wider range of glaciological phenomena than we do.

The ice sheets we concentrate on are kilometers-thick layers of ice covering continental land masses (**Figure 1**). Such ice sheets are currently found in Greenland and Antarctica, and smaller versions termed ice caps exist in the Canadian, Norwegian, and Russian Arctic and on some islands in the Southern Ocean. Ice sheets differ from steeper mountain glaciers in that their flow is less dominated by bedrock topography. Our focus is also entirely on terrestrial ice sheets; we are not concerned with the polar ice caps on Mars or more exotic locales such as the icy shell of the Jovian moon Europa.

Ice sheets are maintained by the net accumulation of snow over a mean annual climate cycle in the center of an ice sheet, where high elevation and possibly higher latitude can contribute to cold surface temperatures. Mass loss may occur owing to net melting near the ice-sheet margins, where lower surface elevation and sometimes lower latitudes can lead to warmer surface temperatures. Ice flows from areas of net accumulation to regions of net mass loss through viscous creep, with the ice sheet spreading under its own weight. Where there is insufficient surface melting or sublimation of ice, ice sheets can also spread to the edge of the continent, where the ice begins to float and can subsequently break off as icebergs. Greenland is an example of an ice sheet that experiences significant marginal melting, whereas Antarctica primarily loses mass through iceberg calving.

The natural evolution timescale for the large-scale geometry of an ice sheet is its advective timescale, given by its horizontal extent divided by ice-flow velocity. Ice velocities can differ markedly, and a unique timescale can be difficult to identify (**Figure 1**) but generally runs to a minimum of hundreds of years, and is often much longer. However, there are also shorter timescales at play. Seasonal variations in surface melting and ocean conditions around ice sheets are observed to have a direct effect on ice-flow velocities, even if large-scale geometry sees only an averaged ice velocity (Zwally et al. 2002). Additionally, diurnal forcing due to tides and surface melt cycles (Bindshadler et al. 2003, Bartholomew et al. 2010) as well the abrupt drainage of ice-dammed water bodies (Das et al. 2008) can affect ice flow. On such short scales, elastic and viscoelastic models have been used to describe observed behavior (Reeh et al. 2003, Tsai & Rice 2010). However, over longer periods exceeding a few days at most, ice flow is almost always modeled as a purely viscous creep. Our review focuses solely on these longer timescales.

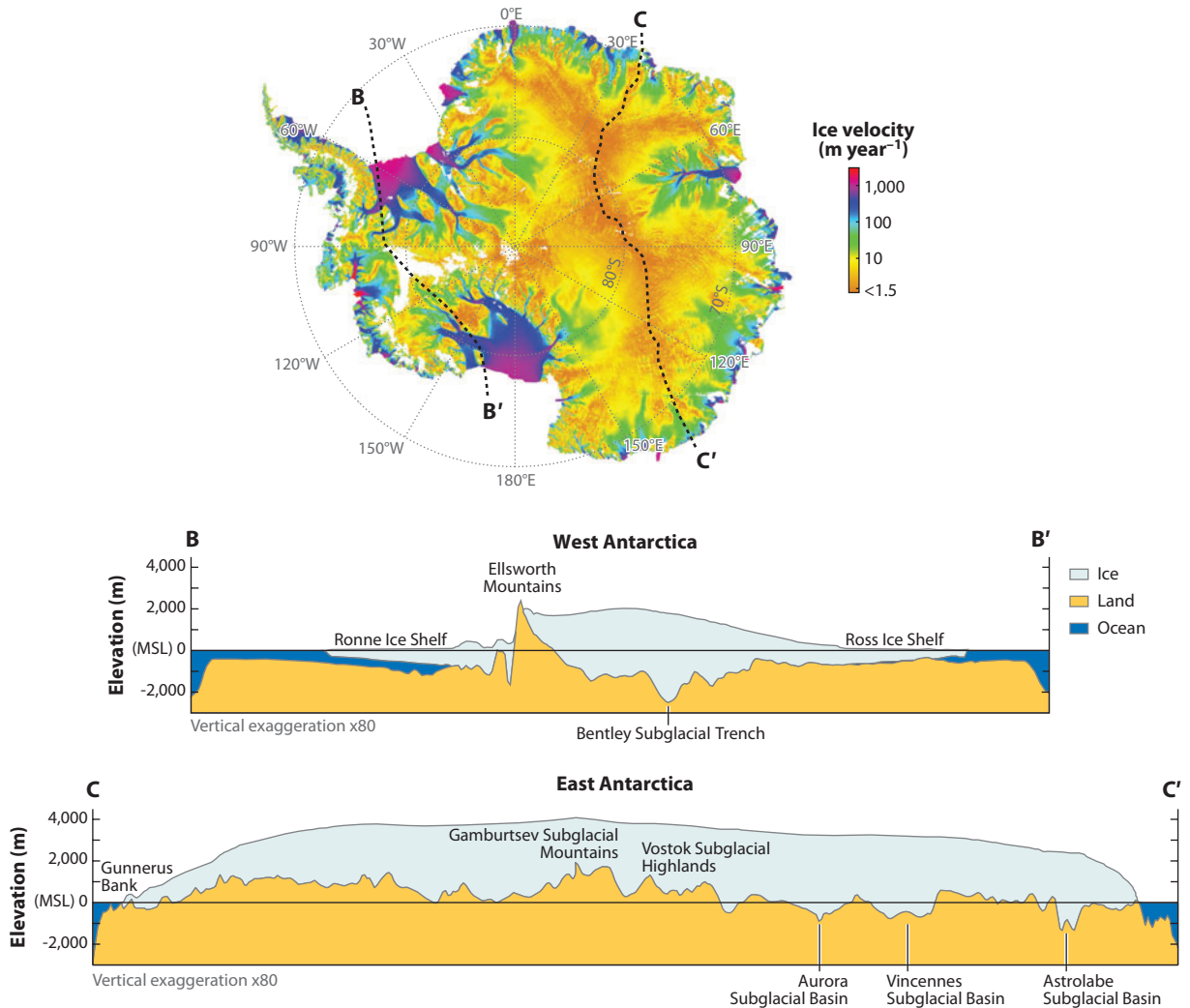


Figure 1

(*Top panel*) Surface velocities in Antarctica, generated from the data set in Rignot et al. (2011). Part of the domain shown consists of floating ice. Clearly visible is the channelized structure of ice-stream flow. (*Bottom panels*) Cross sections of Antarctica, as shown by the lines BB' and CC' in the map. The ice-sheet bed in West Antarctica is mostly below sea level. Cross-sectional images courtesy of Peter Fretwell, British Antarctic Survey, based on the data set described in Lythe et al. (2001). Abbreviation: MSL, mean sea level.

2. ICE FLOW

Most models for ice flow assume a relatively simple rheology with a strain-rate-dependent viscosity. We let $\mathbf{u} = (u_1, u_2, u_3) = (u, v, w)$ be the velocity field in the ice relative to a Cartesian coordinate system $(x_1, x_2, x_3) = (x, y, z)$, with σ_{ij} and τ_{ij} denoting the stress tensor and its deviatoric part, linked through $\sigma_{ij} = \tau_{ij} - p\delta_{ij}$, with $p = -\sigma_{kk}/3$, where we have applied the summation convention. Ice is generally treated as incompressible with (under terrestrial conditions) inconsequential variations in density owing to temperature and impurities:

$$\nabla \cdot \mathbf{u} = 0. \quad (1)$$

Most rheological models for ice posit a standard viscous relationship between deviatoric stress τ_{ij} and strain rate D_{ij} (commonly also denoted $\dot{\epsilon}_{ij}$ in glaciology) of the form

$$\tau_{ij} = 2\eta D_{ij}, \quad D_{ij} = \frac{1}{2} \left(\frac{\partial u_i}{\partial x_j} + \frac{\partial u_j}{\partial x_i} \right), \quad (2)$$

where the viscosity is assumed to depend on the strain rate only through its second invariant $D = \sqrt{D_{ij}D_{ij}/2}$. Observational evidence points to a shear-thinning rheology; the most widely used form is Glen's law, motivated by data fit to a power law in Glen (1958). In standard glaciological notation,

$$\eta = \frac{1}{2} B D^{-1+1/n}, \quad (3)$$

with B independent of the strain rate and n constant. Glen's work indicates $n \approx 3$. This is the most widely used rheological model for ice and is also often expressed in the alternative form $D_{ij} = A\tau^{n-1}\tau_{ij}$, where $\tau = \sqrt{\tau_{ij}\tau_{ij}/2}$ and $A = B^{-1/n}$. Other, more recent work suggests a more complicated relationship between η and D (Goldsby & Kohlstedt 2001), whereas even more complex Reiner-Rivlin and second-grade rheologies that fall outside of the general form given in Equation 2 have also been proposed (McTigue et al. 1985, Man & Sun 1987).

The viscosity of ice is also known to depend on the temperature T , impurity content, and (if the temperature reaches the melting point) the degree of partial melting (i.e., the moisture content). In Glen's law (Equation 3), these dependences are usually absorbed into the prefactor $B = B(T, \dots)$. An Arrhenius-type relationship is usually assumed, of the form (Cuffey & Paterson 2010)

$$B = B_0 \exp(E_0/RT). \quad (4)$$

The Reynolds numbers for typical ice-sheet flows are extremely low, approximately 10^{-12} (Fowler & Larson 1978, Morland & Johnson 1980). An ice sheet therefore behaves as a Stokes flow under the action of gravity, satisfying

$$\frac{\partial \tau_{ij}}{\partial x_j} - \frac{\partial p}{\partial x_i} + \rho g_i = 0, \quad (5)$$

where ρ is the density of ice, and g_i is the component of gravity in the i direction.

Let us assume there is an upper surface in contact with the atmosphere $z = s(x, y, t)$, and a lower surface $z = b(x, y)$ in contact with bedrock or some other substrate (which we call the bed for short), where z is measured vertically upward from sea level (floating ice shelves are discussed in Section 7). We let n_i be an upward-pointing normal to the upper surface (which we call the surface for short) and the bed. Up to an atmospheric gauge pressure, the surface is stress free and behaves as a free boundary:

$$\sigma_{ij}n_j = 0 \quad \text{and} \quad \frac{\partial s}{\partial t} + u \frac{\partial s}{\partial x} + v \frac{\partial s}{\partial y} = w + a, \quad (6)$$

where a is the rate of snow accumulation per unit area, or of melting per unit area if $a < 0$. The bed $z = b(x, y)$ is a material surface with zero normal velocity, assuming negligible melt there. In addition, there may or may not be slip. Most models of ice dynamics assume that slip can be described by a friction law that relates shear stress τ_b at the bed to sliding velocity u_b at the bed, as well as possibly to other state variables that we discuss below, in the form $\tau_b = f(u_b)$. This leads to either $\mathbf{u} = \mathbf{0}$ (no slip) or

$$\mathbf{u} \cdot \mathbf{n} = 0 \quad \text{and} \quad \tau_{jk}(\delta_{ij}n_k - n_i n_j n_k) = f(|\mathbf{u}|)u_i/|\mathbf{u}|, \quad (7)$$

where, by construction, the shear stress vector is parallel to the velocity vector, and tangential to the bed, and has magnitude $f(|\mathbf{u}|)$.

The above ignores complications due to bedrock deformation, which may be significant as the weight of ice sheets is capable of deforming the lithosphere and displacing underlying mantle material. All modern simulation models have a component that computes this bed subsidence.

Sliding is often a dominant component in ice flow (Blankenship et al. 1986, Engelhardt & Kamb 1997), and the choice of constitutive relation $f(u_b)$ can be at least as important as the details of ice rheology. There are, however, much fewer data to support or constrain different possible forms of $f(u_b)$ than there are for rheological relations such as Equation 3, and a greater number of processes are involved in sliding than in ice deformation alone. The no-slip condition $\mathbf{u} = \mathbf{0}$ is frequently used in regions where the bed is below the melting point, although observations show sliding to be possible even at very low temperatures (Cuffey et al. 1999), and Fowler (1986b) suggested that friction laws should explicitly depend on temperature T , varying continuously up to the melting point. For ice at the melting point, when rapid sliding becomes possible, typical friction laws $f(u_b)$ fall into two categories: Either they increase monotonically and without bound in velocity, or they do have an upper bound and are not universally invertible. This distinction has important consequences for the development of thin-film models, described in Section 3.

There are few field data that can constrain the functional form of the friction law f (Sugiyama & Gudmundsson 2004), and most choices are based on theory and laboratory experiments. The original theory of glacier sliding considers ice creep past small-scale roughness at the bed and suggests power laws of the form

$$f(u_b) = C u_b^m, \quad (8)$$

where C depends on the local amount of bed roughness, and $m = 1/n$ (Weertman 1957, Nye 1969, Kamb 1970, Fowler 1981). Depending on the detailed processes involved, exponents other than $1/n$ have also been advocated (Liboutry 1987).

There is evidence that pressurized water under the ice affects sliding in mountain glaciers (Iken & Bindshadler 1986) as well as in Greenland (Zwally et al. 2002) and Antarctica (Engelhardt & Kamb 1997). Theory and experiments attribute this to two different mechanisms. Partial separation of ice from bed roughness (Liboutry 1968) causes friction to depend on the effective pressure N as well as on u , where N is normal stress minus water pressure at the bed. The precise form of the resulting sliding law is uncertain, but viscous-contact-problem models for flow at the roughness scale (Fowler 1986a, Schoof 2005, Gagliardini et al. 2007) suggest

$$f(u_b) = \mu N \tilde{f} \left(\frac{u_b}{A b_r N^n} \right), \quad (9)$$

where μ is a bed roughness slope, b_r is a roughness amplitude, and the function \tilde{f} is bounded; this modeling work, however, is limited to relatively simple bed geometries (Fowler 1987) and ignores transient cavity evolution that could lead to the history-dependent effects evident in Sugiyama & Gudmundsson (2004). An alternative view is motivated by the motion of ice over granular sediments or till. Sliding may then result from deformation of the underlying sediment (Blankenship et al. 1986) and is sometimes referred to as basal motion instead. Boulton & Hindmarsh (1987) popularized an effective-pressure-dependent viscous rheology for till, leading to friction laws of the form

$$f(u_b) = C u_b^a N^b. \quad (10)$$

These are still in widespread use, but more recent work suggests that subglacial till is a Coulomb-plastic material with a yield stress $\tau_c = \mu N$ (Iverson et al. 1998, Tulaczyk et al. 2000a). In that case (Schoof 2006)

$$\begin{aligned} f(u_b) &= \tau_c & \text{when } u_b > 0, \\ |f(u_b)| &\leq \tau_c & \text{when } u_b = 0. \end{aligned} \quad (11)$$

Frequently, this is also regularized as $f(u_b) = \tau_c u_b / \sqrt{u_b^2 + \varepsilon^2}$ (Bueler & Brown 2009), which reproduces Equation 11 in the limit of small ε . Alternatively, Equation 9 can also motivate a regularized friction law (see, e.g., Schoof 2010a).

The above indicates that sliding behavior can be highly dependent not only on bed temperature, but also on effective pressure, and comprehensive ice-sheet models require a prescription not only for T , but also for N .

3. THIN-FILM MODELS

Notwithstanding their importance, a great deal of basic insight can be obtained by ignoring the additional state variables N and T , focusing purely on the basic Stokes-flow model. Primary interest in glaciology is typically in the evolution of surface geometry (which represents ice volume and extent, and therefore holds greatest physical interest) as well as of ice-flow velocities (which are more readily measured than meaningful changes in geometry s , as the timescale for significant changes in s is long compared with the instrumental record).

In very few cases is the model above ever solved as stated [and if so, this has to be done numerically (see, e.g., Jouvett et al. 2008)]. The basis of most practical ice-sheet models is the low aspect ratio ($\sim 10^{-2}$ – 10^{-3}) of terrestrial ice sheets. The most widely used model over time has been a classical lubrication approximation (Fowler & Larson 1978, Morland & Johnson 1980, Hutter 1983) often termed the shallow-ice approximation.

3.1. Shallow-Ice Models

For the model in Section 2, a lubrication approximation requires that the friction law $\tau_b = f(u_b)$ be invertible to give a sliding law $u_b = F(\tau_b)$. This is possible for the power law (Equation 8) but not for bounded friction laws such as Coulomb friction (Equation 11). Assuming a power-law rheology (Equation 3), the shallow-ice approximation reduces the Stokes-flow model of Section 2 to

$$\frac{\partial \boldsymbol{\tau}}{\partial z} = -\nabla_x p, \quad \frac{\partial p}{\partial z} = -\rho g, \quad \frac{\partial \mathbf{U}}{\partial z} = 2A|\boldsymbol{\tau}|^{n-1}\boldsymbol{\tau} \quad \text{on } b < z < s,$$

$$\boldsymbol{\tau} = \mathbf{0}, \quad p = 0 \quad \text{on } z = s, \quad \mathbf{U} = F(|\boldsymbol{\tau}|\boldsymbol{\tau}/|\boldsymbol{\tau}|) \quad \text{on } z = b, \quad (12)$$

where $\boldsymbol{\tau} = (\tau_{xz}, \tau_{yz})$, $\mathbf{U} = (u, v)$, and $\nabla_x = (\partial/\partial x, \partial/\partial y)$. The depth-integrated mass-conservation equation arising from Equation 1 is

$$\frac{\partial s}{\partial t} + \nabla_x \cdot \mathbf{q} = a, \quad \mathbf{q} = \int_b^s \mathbf{U} dz,$$

with Equation 12 yielding

$$\mathbf{U} = -2(\rho g)^n \left[\int_b^{dz} A(dz')(s - dz')^n dz' \right] |\nabla_{x's}|^{n-1} \nabla_{x's} - F(\rho g(s - b)|\nabla_{x's}|) \frac{\nabla_{x's}}{|\nabla_{x's}|}. \quad (13)$$

A simpler special case arises for no slip ($F = 0$), with A a constant:

$$\frac{\partial s}{\partial t} - \nabla_x \cdot \left[\frac{2A}{n+2} (s - b)^{n+2} |\nabla_{x's}|^{n-1} \nabla_{x's} \right] = a.$$

Ignoring any additional state variables in A and F , Equation 13 is essentially a highly nonlinear diffusion problem for surface elevation $s(x, y, t)$ (flux is an increasing function of gradient $-\nabla_{x's}$); this is typically the quantity of primary interest in ice-sheet modeling.

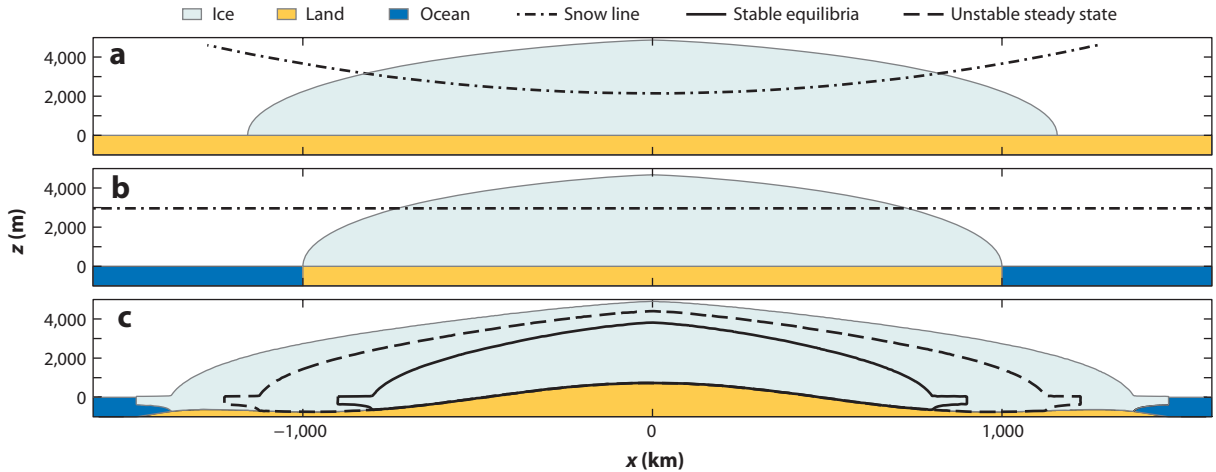


Figure 2

Three different flavors of steady shallow ice sheets. (*a,b*) The surface experiences net accumulation when above the snow line (*dotted-dashed line*) and net melting below. In panel *a*, there is more melting with distance from the origin, and this determines the steady-state margin position. In panel *b*, the snow line is flat, and ice covers the entire continental land mass. In panels *a* and *b*, the ice-free state is also a viable steady state. (*c*) A marine ice sheet (Section 7), with no surface melting but with multiple equilibria generated by an overdeepened bed. Solid lines correspond to stable equilibria, and the dashed line is an unstable steady state.

A sometimes weakly perceived point in glaciology is that the model above is in fact a free-boundary problem: Equation 13 holds only in the ice-covered part of the domain (defined by $s - b > 0$) in the (x, y) plane. At the free boundary of the ice-covered domain, with $\mathbf{n}_x = (n_x, n_y)$ as its normal, we have vanishing flux and thickness, $\mathbf{q} \cdot \mathbf{n}_x = 0$ and $s - b = 0$. In the ice-free domain (defined by $s = b$), we have growth of the ice cover only if the accumulation rate is positive. With $\mathbf{q} = \mathbf{0}$ in the ice-free region, this allows us to put there

$$\frac{\partial s}{\partial t} = \frac{\partial s}{\partial t} + \nabla_x \cdot \mathbf{q} \geq a. \quad (14)$$

This free-boundary problem is amenable to modern variational analysis (Calvo et al. 2002, Jouvet et al. 2011); the one-dimensional steady-state version is also amenable to solution by shooting-type ordinary-differential-equation methods based on a change of variable (e.g., Jouvet et al. 2011).

The free-boundary, shallow-ice model above has several noteworthy properties. Let us consider a steady climate in which a may depend on surface elevation but not explicitly on time. The canonical behavior is then one of diffusive relaxation toward steady states (Fowler 2001). When $a = a(x, y, s(x, y, t))$ increases with surface elevation s , multiple stable steady states are also possible. This simply results from a positive feedback between the surface elevation and the possibility of having net accumulation (because of colder temperatures at altitude) rather than net ablation, which can lead to the same function $a(x, y, s(x, y))$ supporting a stable ice sheet or the complete absence of an ice sheet ($s \equiv b$ everywhere; **Figure 2**). Under changes in climate, hysteresis is then possible (Oerlemans 1981): An existing ice sheet can survive a rising snow line far beyond the point at which the growth of a new ice sheet would be initiated on the bare land surface. Jouvet et al. (2011) further showed that, if the snow-line elevation does not depend on position, so $a = a(s(x, y, t))$, then a steady ice sheet necessarily occupies the entire land mass.

3.2. Membrane Models

A shallow-ice model assumes an invertible friction law or no slip; otherwise the model will not work: Equation 12 predicts that shear stress at the bed $\boldsymbol{\tau} = -\rho g(s-b)\nabla_{\mathbf{x}}s$ is determined purely geometrically and must be balanced by friction $f(|\mathbf{U}|)\mathbf{U}/|\mathbf{U}|$ there. This defines the sliding velocity implicitly. This inversion will not work, for instance, for the Coulomb friction law (Equation 11).

Even if the sliding law is invertible, a lubrication model may be inappropriate when sliding is rapid, as some of the stress components ignored in Equation 12 can become large; this effect can be characterized in terms of a slip ratio or stress ratio (Hindmarsh 1993, Schoof & Hindmarsh 2010). For rapid sliding, a so-called membrane model may become necessary instead of a shallow-ice model. This is also a depth-integrated model, but with the crucial difference that vertical shearing is treated as negligible, while extensional stresses and lateral shear stresses feature at leading order in the force balance.

We let indices a and b range over $(1, 2)$ only so that x_a and U_a are subscript notation for horizontal position (x, y) and velocity components $\mathbf{U} = (u, v)$. A membrane model assumes a plug flow in the vertical, so \mathbf{U} is independent of z . A horizontal strain rate \tilde{D}_{ab} can be defined by analogy with Equation 2, $\tilde{D}_{ab} = (\partial U_a/\partial x_b + \partial U_b/\partial x_a)/2$. A membrane stress can then be defined in invariant form as $T_{ab} = 2b\eta(D_{ab} + D_{cc}\delta_{ab})$, where $b = s - b$ is the ice thickness. Explicitly,

$$\mathbf{T} = \begin{pmatrix} T_{xx} & T_{xy} \\ T_{yx} & T_{yy} \end{pmatrix} = \begin{pmatrix} 2\eta b \left(2\frac{\partial u}{\partial x} + \frac{\partial v}{\partial y} \right) & \eta b \left(\frac{\partial u}{\partial y} + \frac{\partial v}{\partial x} \right) \\ \eta b \left(\frac{\partial u}{\partial y} + \frac{\partial v}{\partial x} \right) & 2\eta b \left(2\frac{\partial v}{\partial y} + \frac{\partial u}{\partial x} \right) \end{pmatrix}, \quad (15)$$

where T_{xx} and T_{yy} are usually referred to as extensional or longitudinal stresses, and $T_{xy} = T_{yx}$ as the lateral shear stress. A membrane model now takes the form

$$\frac{\partial T_{ab}}{\partial x_b} - f(|\mathbf{U}|)U_a/|\mathbf{U}| - \rho g b \frac{\partial s}{\partial x_a} = 0, \quad (16)$$

where η is still the ice viscosity here. Its dependence on the strain rate must now be computed by replacing the second invariant of the three-dimensional strain rate D by the invariant \tilde{D} , where $\tilde{D}^2 = \tilde{D}_{ab}\tilde{D}_{ab}/2 + (\tilde{D}_{aa})^2/2$, and by averaging material properties over the ice thickness. For instance, Equation 3 becomes $\eta = 2^{-1}\tilde{B}\tilde{D}^{-1+1/n}$, where \tilde{B} is the mean of B taken over the ice thickness. Ice geometry evolves as

$$\frac{\partial b}{\partial t} + \nabla_{\mathbf{x}} \cdot (b\mathbf{U}) = a. \quad (17)$$

Although it has the advantage of brevity and simplifying numerical analysis (Schoof 2006), the invariant notation of Equation 16 is not used universally in glaciology, in which the equation is usually written out component-wise. Membrane models were originally derived for floating ice shelves (e.g., Morland & Shoemaker 1982, Morland 1987, Morland & Zainuddin 1987) for which the basal shear stress is zero, and are analogous to free-film models elsewhere in fluid dynamics (DiPietro & Cox 1979). They were first applied to rapid sliding ice by Muszynski & Birchfield (1987) and MacAyeal (1987). Because of their association with ice shelves and rapidly sliding ice streams, membrane models have often been referred to as shelfy stream models in glaciology. Attempts have also been made to create hybrid thin-film models (somewhat inaccurately termed higher-order models) combining the shear-dominated dynamics of slow sliding in the lubrication flow model with the ability of membrane models to capture fast sliding. The earliest attempt is probably due to Herterich (1987); extended to three dimensions, this has become known as the Blatter-Pattyn model (Blatter 1995, Pattyn 2003). The Herterich-Blatter-Pattyn model requires the vertical dimension to be resolved, and depth-integrated alternatives have recently appeared

(Hindmarsh 2004a, Schoof & Hindmarsh 2010, Goldberg 2011). For a detailed asymptotic analysis and a review of the relationship between different thin-film approximations, readers are referred to Schoof & Hindmarsh (2010). The elliptic structure of Equation 16 and related hybrid models has spawned a literature on their numerical analysis (Glowinski & Rappaz 2003, Rappaz & Reist 2005, Schoof 2010a).

4. THERMOMECHANICAL EFFECTS

The discussion of ice viscosity and sliding behavior above indicates that the temperature T plays a critical role in ice-sheet dynamics. Most ice-sheet models solve for the temperature equation in three dimensions, even if using a thin-film ice-flow model. Advection, conduction, and strain heating are all typically important:

$$\rho c \frac{\partial T}{\partial t} + \rho c \mathbf{u} \cdot \nabla T = k \nabla^2 T + \tau_{ij} D_{ij}, \quad (18)$$

where c is the heat capacity, k is the thermal conductivity, and $\tau_{ij} D_{ij}$ is viscous dissipation. For thin-film models, the full diffusion term $-k \nabla^2 T$ is often replaced by diffusion $-k d^2 T / dz^2$ in the vertical direction alone. Realistic boundary conditions involve complicated energy-balance processes at the bed and surface, including radiative, sensible, and turbulent heat fluxes, as well as phase changes. The simplest models prescribe the surface temperature $T = T_s$, while the bed either is at the melting point, $T = T_m$, or is cold with $T < T_m$, and the temperature gradient must match a prescribed geothermal heat flux $-k \nabla T \cdot \mathbf{n} = G$.

The heat equation (Equation 18) assumes that the ice is below the melting point. However, dissipation allows regions of temperate ice to form, where $T = T_m$ and conservation of energy leads to an equation for moisture content rather than temperature. Ice viscosity is then potentially a sensitive function of moisture content (Duval 1977, Lliboutry & Duval 1985). Ignoring the pressure dependence of the melting point and employing a Boussinesq approximation, one can write the moisture equation approximately as (see also Fowler 1984)

$$\rho L \left[\frac{\partial \omega}{\partial t} + \mathbf{u} \cdot \nabla \omega + \nabla \cdot \mathbf{j} \right] = \tau_{ij} D_{ij}. \quad (19)$$

Here ω is the mass fraction of water, and $\mathbf{j} = \omega(\mathbf{u}_w - \mathbf{u})$ is moisture flux, where \mathbf{u}_w is the water velocity. A constitutive law is required to describe \mathbf{j} ; Darcy's law puts $\mathbf{j} = (\kappa/\eta_w)(\rho_w \mathbf{g} - \nabla p_w)$, where κ , η_w and p_w are the ice permeability, water viscosity and water pressure, respectively. With this, a further relation for p_w based on the compaction of the ice matrix becomes necessary to close the problem (see, e.g., Fowler 2001), and if significant drainage occurs, the continuity equation for the ice matrix (Equation 1) must also be modified to account for the mass loss. In practice, most current ice-sheet simulations do not solve the equation above but effectively remove any excess water once a critical moisture content is reached (approximately 1%–3%).

Greve (1997) treated temperate and cold ice separately, explicitly locating the cold-temperate transition surface that divides them. Alternatively, the two cases can be combined by writing them in terms of the enthalpy of the ice-moisture mixture, and numerical methods that adopt this approach have recently been developed (Aschwanden & Blatter 2009, Aschwanden et al. 2012).

4.1. Thermally Induced Oscillations

The paleoclimate record indicates abrupt discharges of ice from ice sheets during at least the most recent ice age (Hemming 2004), and some valley glaciers are similarly known to surge; that is, they

undergo often abrupt and quasi-periodic increases in flow velocity, during which they lengthen and thin, only to return to a more slowly flowing quiescent state in which they shorten and thicken (Kamb et al. 1985, Frappé & Clarke 2007). This represents a major departure from the picture of diffusive relaxation to a steady state described above.

Robin (1955) suggested that a feedback between strain heating and softening ice at higher temperatures could result in a surge through a thermal runaway process. Modeling parallel-sided slabs of ice with a temperature-dependent viscosity of the form given in Equation 4, Clarke (1977) observed that some combinations of thickness and inclination allow for multiple thermal states, namely a cold and hence slowly flowing state, as well as a warm and therefore fast state. An increase in ice thickness or surface slope could then result in the slow state ceasing to exist, forcing the ice sheet into the fast state, and conversely a decrease in thickness or slope could lead to the fast state disappearing, so the resulting switches between the fast and slow branches could explain surges.

In reality, matters are more complicated. These multiple thermal states are associated with a prescribed ice geometry and effectively assume that the temperature evolves on a fast timescale compared with ice geometry; in practice, this is not the case. Taking the opposite point of view, Fowler & Larson (1980a,b) argued that, in the absence of advection, one can compute unique stable steady states to the thermomechanical shallow-ice problem and that the ice sheet will settle into this state rather than undergo oscillations. Moreover, the warm state may not necessarily be physical: Fowler et al. (2010) considered a setting in which dissipation is concentrated near the bed and showed that there are then no coexisting cold and warm states, as the latter would require temperatures above the melting point; instead, there is a continuous progression from a cold to a temperate ice state.

Sliding potentially makes multiple thermal states easier to construct. When sliding is activated at the melting point, coexisting cold and warm states can be constructed straightforwardly if we concentrate on the limit of conduction-controlled temperatures. With a surface temperature T_s , the temperature profile is then either $T = T_s + G(s - z)/k$ if the bed is cold or $T = T_s + (T_m - T_s)(s - z)/b$ otherwise. The former is viable if the temperature at the bed is below T_m , so $b < (T_m - T_s)k/G$, whereas, in the absence of other sources of heat, the latter requires the sum of geothermal and frictional heating to exceed conduction into the ice, so $G + \tau_b u_b > (T_m - T_s)k/b$. Because dissipation $\tau_b u_b$ is intrinsically positive, there is therefore a range of values $(T_m - T_s)k/(G + \tau_b u_b) < b < (T_m - T_s)k/G$ (depending on the precise friction law) for which both fast and slow sliding is possible. Oscillations could then presumably be explained theoretically using a spatially extended relaxation oscillator, as in Fowler (1989), although the implied separation of timescales may not be warranted as above.

Using a shallow-ice model in which sliding according to Equation 8 is activated discontinuously when $T = T_m$ at the bed, Payne (1995) found periodic oscillations of a planar ice sheet (i.e., with one horizontal dimension). This is essentially the same as the binge/purge oscillation in MacAyeal (1993), and similar results from a variety of models have been reported (e.g., Calov et al. 2010, van Pelt & Oerlemans 2012).

Discontinuous sliding in shallow-ice models is, however, problematic, and numerical results have often been less than robust: This is because the horizontal ice velocity u then changes discontinuously while the vertical ice velocity is effectively indeterminate, and the advection term in Equation 18 goes awry at the transition from cold- to warm-based ice (Bueler & Brown 2009). Either a boundary-layer description (Barcilon & MacAyeal 1993) becomes necessary to model this transition (but this has not been fully developed) or the transition from no slip to sliding as a function of temperature must be regularized (Fowler 1986b).

We note that this discussion relates purely to thermally controlled sliding. In reality, melt-water production may also have a significant impact on sliding, as discussed in Section 6.

4.2. Thermally Induced Streaming

The velocity field of large sheets typically exhibits strong patterning (**Figure 1**), with prominent bands of fast flow called ice streams. These features are sometimes associated with pronounced bedrock troughs, but in other cases they have no strong association with the underlying bed topography. This has naturally led to the question of whether ice streams could be the result of a thermoviscous fingering instability.

With many of the same caveats as above, one can conceive of multiple thermal states, as in Section 4.1, leading to patterning. With the same parallel-sided slab geometry used by Clarke (1977), and with a shallow-ice model coupled with the shallow form of the heat equation (Equation 18) in which $-k\nabla^2 T$ is replaced by $-kd^2 T/dz^2$, such patterning would be easy to construct. If the combination of ice thickness and inclination is such as to allow multiple thermal states, then they can clearly coexist spatially: Let us suppose that the x and y axes point down- and cross-slope, respectively. If flow is purely in the x direction, the modified version of the heat equation does nothing to prevent discontinuities in T across streamlines (lines of constant y), and neither does the shallow-ice approximation, so the warm and cold states can coexist side by side.

As above, this is somewhat contrived because it relies on a fixed geometry and hence a fast temperature timescale. However, the argument already points to a potential issue in thermomechanical shallow-ice models, suggesting possible lateral discontinuities in velocity. More sophisticated models including such effects as lateral diffusion of heat (which is only relevant at scales comparable to ice thickness) or lateral shear stresses are required to prevent this.

In numerical simulations with shallow-ice models, radially symmetric solutions are indeed sometimes unstable to fingering [usually referred to as the formation of spokes (see Payne & Dongelmans 1997)]. This can occur even with no basal sliding, when discontinuities in heat advection owing to the abrupt initiation of sliding are not an issue (Payne et al. 2000, EISMINT experiment F). However, these numerical “solutions” of the shallow-ice problem are problematic, as they invariably exhibit dependence on grid spacing and on the details of the discretization (Payne et al. 2000, Payne & Baldwin 2000, Hindmarsh 2004b, Saito et al. 2006, Bueller et al. 2007, Calov et al. 2010). In view of our comment above (although this is based on an idealized geometry), grid dependence is not surprising, as shallow-ice models lack a mechanism to suppress short-wavelength velocity variations. Indeed, Hindmarsh (2004b, 2006b, 2009, 2011) argued that, even in the absence of sliding, the thermomechanical shallow-ice models allow for undamped growth of transverse short-wavelength modes, suggesting that such models are in fact ill-posed.

Nevertheless, the physical instability appears to be robust: Hindmarsh (2006b) conducted a numerical linear stability analysis of both shallow-ice and membrane models; instability is predicted in both cases, but lateral stresses dampen the problematic growth of short wavelengths. A fully developed fingering instability with a membrane model appears to converge under grid refinement (Hindmarsh 2009), lending support to the conclusion that the phenomenon is genuine. The picture that emerges somewhat tenuously from the literature is that a unique one-dimensional steady state as conceived of by Fowler & Larson (1980a,b) can apparently be linearly unstable to transverse perturbations (Hindmarsh 2004b), and the subsequent evolution should lead to fast ice flow in a finite domain drawing down the surface locally and thereby entraining ice from neighboring cold regions (Payne & Dongelmans 1997), which may limit further growth of the instability. In the fully developed state, the streams then evolve so that their spacing reflects their capacity to carry away the discharge from the surrounding catchment basin (Hindmarsh 2009).

There remain significant uncertainties, however, and neither theory nor numerical simulations can as yet robustly predict the onset of either fingering or oscillatory behavior, or their subsequent evolution. Realistic ice-sheet simulations commonly report both streaming and oscillations, and it is important to distinguish which features are robust and which are numerical artifacts. A number of related geophysical problems exhibit similar thermoviscous fingering (Helfrich 1995, Balmforth & Craster 2000), but the details of the flow and thermal boundary conditions are sufficiently different to make direct comparison not particularly helpful.

5. DRAINAGE

In the discussion above, sliding is generally associated purely with the temperature reaching the melting point. In reality, heat fluxes and dissipation continue to affect sliding through water production even when T_m has been reached. Water is generally assumed to enter into the friction law through the effective pressure N , and this is ultimately set by the storage and drainage of water along the bed.

Subglacial drainage is a substantial subject of its own but has largely been given short shrift in ice-sheet modeling. This is partly a result of a dearth of reliable data to constrain the numerous constitutive relations that must be defined. We review the relevant concepts only briefly here.

Most models, if they are not entirely hypothetical, are based on observed mountain glacier hydrology, with the relevant physics assumed to carry over to large ice sheets (Fountain & Walder 1998). This is most realistic for the margins of the Greenland ice sheet: As on most mountain glaciers, surface melt water is able to reach the bed there. The interior of Greenland and the whole of Antarctica have basal water supplies limited by geothermal heat fluxes and dissipation in the ice and at the bed, which leads to melt rates typically orders of magnitude smaller than those generated by surface melting.

On undeformable bedrock, two standard models are linked cavities, connected void space resulting from the same partial ice-bed separation that reduces friction due to bed roughness (see Walder 1986, Kamb 1987), and R othlisberger channels, incised into the ice due to the frictional heating of the water flowing through them (R othlisberger 1972). On deformable and erodible beds, such channels are still thought to form, but they may also be incised downward into erodible sediments (Walder & Fowler 1994). Drainage may also occur within the till (Alley et al. 1986, Bougamont et al. 2003) or in some form of a patchy “sheet” at the ice-till interface (Alley 1989, Flowers & Clarke 2002, Creyts & Schoof 2009, Hewitt 2011), which may in fact consist of linked cavities that form behind larger rocks within the till. The distinction between these different alternatives is not clear-cut.

Drainage models can be divided into two categories: distributed and channelized. In distributed models, continuum descriptions replace models of individual conduits. This is feasible for linked cavities, water sheets, and flow through till, but not for individual R othlisberger channels that tend to be isolated from one another or form an arborescent drainage structure. Here we focus only on distributed systems; models that combine these with channelized drainage elements have only recently been proposed (Schoof 2010b, Hewitt 2011) and are still in development, although they must clearly be relevant to the margins of the Greenland ice sheet (Bartholomew et al. 2010).

Defining h_w as an average water depth (average volume of water per unit area of the bed), and \mathbf{q}_w as the average (two-dimensional) water flux, the conservation of basal water can be written as

$$\frac{\partial h_w}{\partial t} + \nabla_x \cdot \mathbf{q}_w = m + \frac{1}{\rho L} (G + k \nabla T \cdot \mathbf{n} + \tau_b u_b + |\mathbf{q}_w \cdot \Psi|), \quad (20)$$

where m is the supply of water from the ice surface and from any temperate ice above the bed, and the remaining terms arise from melting at the bed: L is the latent heat, G the geothermal heat flux, $-k\nabla T \cdot \mathbf{n}$ the conduction into the ice, $\tau_b u_b$ the frictional heating, and $|\mathbf{q}_w \cdot \Psi|$ the dissipation in the water flow. $\Psi = -\rho g \nabla_x s - (\rho_w - \rho)g \nabla_x b + \nabla_x N$ is the hydraulic potential gradient driving the flow, and a frequently assumed relationship is

$$\mathbf{q}_w = \kappa(b_w)\Psi, \quad (21)$$

where $\kappa(b_w)$ is a hydraulic transmissivity (e.g., Clarke 2005). To close the problem, one possibility is to assume a general poroelastic relationship $b_w = b_w(N)$ (e.g., Tulaczyk et al. 2000b, Flowers & Clarke 2002); the drainage equation (Equation 20) then becomes an advection-diffusion equation for N [or a hyperbolic problem if $\nabla_x N$ is dropped from the definition of Ψ (see Le Brocq et al. 2009)]. A slightly different class of models posits that water depth evolves according to a local ordinary differential equation $\partial b_w / \partial t = v(u_b, b_w, \Psi, N)$ (Creys & Schoof 2009, Hewitt 2011), in which case Equation 20 is elliptic in N . As this variety of options clearly suggests, there is considerable uncertainty about the dynamics of the drainage system, and much theorizing is done in the relative absence of data.

6. ICE STREAMS

Although thermoviscous fingering (Section 4.2) has been appealed to as an explanation for ice streams, some ice streams are known to flow almost entirely by basal sliding (Engelhardt & Kamb 1997), and this sliding motion can change direction and speed (Siebert et al. 2004, Hulbe & Fahnestock 2007) or even cease altogether without the bed actually freezing (Retzlaff & Bentley 1993, Catania et al. 2003), pointing to subglacial drainage as a crucial factor (Anandakrishnan & Alley 1997).

Modeling preoccupations here have been very similar to those discussed in Section 4: Can positive feedbacks account for temporal variability and patterning? The basic feedback is now that a drop in N leads to a drop in basal drag τ_b , and consequently an increase in sliding velocity u_b . This in turn can lead to an increase in dissipation $\tau_b u_b$, which generates more water, in turn further lowering N and so on. Theories for this come in two slightly different flavors, with little constraint from actual data: a drained view in which the dependence of water discharge on N is key (Fowler & Johnson 1996, Fowler & Schiavi 1998) and an undrained view in which the effect of N on water storage at the bed is of primary importance (van der Veen & Whillans 1996, Tulaczyk et al. 2000b, Sayag & Tziperman 2008, Bougamont et al. 2011). The positive feedback requires either that water discharge increases with decreasing N (as is the case in Section 5 if κ decreases with N) or equally that water storage increases with decreasing N .

To illustrate how this affects patterning in published models, we consider a membrane model (Equation 16) for a parallel-sided inclined slab of ice with the y axis transverse to the slope [so b is constant, $s = s(x)$ with $\rho g b \partial s / \partial x = f_0 = \text{constant}$, $N = N(y)$, $u = u(y)$, and $v = 0$, $T = T(z)$ in the ice] (Hindmarsh 2006b, Sayag & Tziperman 2008). Using the model in Section 5 with $b_w = b_w(N)$,

$$\frac{\partial}{\partial y} \left(b \eta \frac{\partial u}{\partial y} \right) - f(u, N) + f_0 = 0, \quad \frac{\partial b_w}{\partial t} + \frac{\partial}{\partial y} \left(\kappa \frac{\partial N}{\partial y} \right) = \frac{1}{\rho L} \left(G + k \frac{dT}{dz} + f(u, N)u \right). \quad (22)$$

A linear stability analysis of a uniform solution $u \equiv u_0 = \text{constant}$, $N \equiv N_0 = \text{constant}$ [where $f(u_0, N_0) = f_0$] with $f_u := \partial f / \partial u|_{u=u_0}$, $f_N = \partial f / \partial N|_{N=N_0}$, $b_{w,N} = \partial b_w / \partial N|_{N=N_0}$, and η and κ constant produces a dispersion relation for perturbed modes $N = N_0 + N' \exp(iky + \omega t)$,

$u = u_0 + u' \exp(iky + \omega t)$, of the form

$$\sigma = \frac{1}{b_{w,N}} \left(\kappa k^2 - \frac{1}{\rho L} \frac{f_N f_0 - f_N u_0 b \eta k^2}{f_u + b \eta k^2} \right). \quad (23)$$

With the minimal assumption $f_u > 0$, $f_N > 0$, and $b_{w,N} < 0$, we see unconditional instability above a minimum wavelength [controlled by a combination of drainage (κ) and lateral shearing (η)] but no wavelength selection at long wavelengths. The above is for the undrained picture. To reconcile the model with Fowler & Johnson (1996), one would instead insist on κ decreasing with N and allow slow variations in the downstream direction x but assume that no water is stored at the bed. This would lead to the time derivative of b_w being replaced by $\partial[\kappa(N)\Psi_0]/\partial x$, so the downstream coordinate appears as a timelike variable. The effect is the same, however, and we still have instability without wavelength selection. To explain the eventual shutdown of an ice stream, and potentially oscillatory behavior, one needs to account also for the change in ice temperature that results from changes in ice depth in three dimensions.

Further modeling issues arise because the nonlinear evolution of the instability can easily lead to zero water content in the bed (see, e.g., Díaz et al. 2007 for Fowler & Johnson's model); the same can also be inferred from numerical solutions of Sayag & Tziperman's model. We expect sharp boundaries to form between frozen regions (where the membrane model ceases to hold) and ice streams, and these are evident in real ice streams as shear margins (Harrison et al. 1998). Shear margins are a boundary layer in which a Stokes-flow problem must be solved (Raymond 1996, Jacobson & Raymond 1998, Schoof 2004). The physics that controls the subsequent evolution of the margin is not understood, but stress concentration that leads to intense heat dissipation and the possible formation of temperate ice (Jacobson & Raymond 1998, Schoof 2004) is likely to be involved. This is an area of ongoing research.

7. MARINE ICE SHEETS

Some ice sheets can occupy an entire continental land mass and extend as a floating ice shelf onto the surrounding ocean. In this case, we refer only to the part of the ice in contact with the underlying bedrock as the ice sheet and to the remainder as an ice shelf. Typically, the sheet extends into areas where bedrock is below sea level, and the shelf forms only where ice has become sufficiently thin to float. In locations where an ice sheet is grounded largely below sea level, it is referred to as a marine ice sheet; the West Antarctic Ice Sheet is the most prominent example of a marine ice sheet currently in existence (Alley & Bindschadler 2001) (**Figure 1**). The contact line between the sheet and shelf is usually called the grounding line. Its location is generally not fixed but can evolve, so one expects a free-boundary problem to describe the dynamics of marine ice sheets.

Floating ice shelves experience negligible tangential traction at their lower as well as upper boundary. In addition, they are nearly afloat in the Archimedean sense, except possibly very near the grounding line. Their flow is effectively buoyancy driven because of the tendency of a lighter "fluid" (ice) to spread on a denser fluid (ocean water). The appropriate model is the membrane model (Equations 16 and 17) with zero basal traction f , and with b now linked to the surface elevation by Archimedean flotation through $\rho_w(b - s) = \rho b$, where ρ_w is the density of seawater (Shumskiy & Krass 1976, Morland & Shoemaker 1982, Morland 1987, Morland & Zainuddin 1987):

$$\frac{\partial T_{ab}}{\partial x_b} - \rho \left(1 - \frac{\rho}{\rho_w} \right) g b \frac{\partial b}{\partial x_a} = 0, \quad \frac{\partial b}{\partial t} + \nabla_{\mathbf{x}} \cdot (b\mathbf{U}) = a. \quad (24)$$

The ice shelf usually ends at a calving front, where icebergs break off. At this boundary, ice thickness is generally nonzero, and this engenders an imbalance between hydrostatic (or cryostatic) stresses

in ice and water that must be balanced by a nonzero deviatoric extensional stress. This takes the form

$$T_{ab}n_b = \frac{1}{2}\rho \left(1 - \frac{\rho}{\rho_w}\right) g b^2 n_a, \quad (25)$$

where n_a indicates the components of the normal \mathbf{n}_x to the calving front in the (x, y) plane (Shumskiy & Krass 1976, Muszynski & Birchfield 1987, MacAyeal & Barcilon 1988). To evolve the location of the calving front, one must have a second condition describing the rate at which ice breaks off; this is currently the subject of intensive research (e.g., Winkelmann et al. 2011, Benn et al. 2007).

7.1. Sheet-Shelf Coupling

The primary interest in shelves from a large-scale ice dynamics and climate perspective lies in their coupling with the grounded ice sheet rather than in the shelf itself: The melting of ice shelves has a negligible effect on sea levels by Archimedes' principle. Early interest focused on coupling an ice shelf model (Equation 24) to a shallow-ice model (Equation 14) with no slip in one dimension. The force-balance part of the shelf problem in Equation 24, together with the boundary condition in Equation 25 in one dimension, leads to the conclusion that $T_{xx} = 4\eta b \partial u / \partial x = \rho(1 - \rho/\rho_w) g b^2 / 2$ throughout the shelf domain, and the extensional stress is therefore a function of local ice thickness alone.

Chugunov & Wilchinsky (1996) and Wilchinsky & Chugunov (2001) were the first to use matched asymptotics systematically to couple a no-slip shallow-ice flow to a shelf, demonstrating that a Stokes-flow problem must be solved in a boundary layer between the sheet and shelf. Although the reader will be hard-pressed to find an explicit statement to this effect in their papers, their key results amount to the following relationship between the flux q and thickness h_g at the grounding line:

$$q = k A (\rho g)^n h_g^{n+2}, \quad (26)$$

where the dimensionless constant k depends only on n , on the density ratio ρ/ρ_w , and on a modified flotation condition

$$h_g = b|_{x=x_g} = -\tilde{k} \frac{\rho_w}{\rho} b, \quad (27)$$

where \tilde{k} also depends on n and ρ/ρ_w . [Strictly speaking, this flotation thickness must also be small compared with the ice thickness inland to match successfully (see also Schoof 2007b, section 3).] These results mimic more ad hoc ones obtained earlier by Weertman (1974).

A lucid discussion of Chugunov & Wilchinsky's grounding-line boundary-layer problem has been given by Fowler (2011, section 10.2.7). Omitting the rescaled "fast" grounding-line migration rate \dot{x}_G (which should be small) from Fowler's model, one obtains a problem containing the single parameter $\Lambda \propto q / [A(\rho g)^n h_g^{n+2}]$. If, and this is conjecture, this problem possesses a solution only for a unique value of this parameter, this retrieves Equation 26. However, the numerical solutions in Nowicki & Wingham (2008) suggest that Λ (or, equally, the constants k and \tilde{k}) may not in fact be unique but must instead lie within a small range. The key to this appears to lie in contact inequalities (which do not appear in Chugunov & Wilchinsky's work) that must be satisfied on either side of the contact line, and possibly in the complete absence of sliding. Nowicki & Wingham's results suggest that discharge through the grounding line may in some situations be history dependent, as already envisaged by Hindmarsh (1993). However, presently these results are purely numerical, and further work is required.

The case of fast sliding is somewhat easier to deal with than the no-slip-to-shelf transition, as one can now use structurally similar sets of equations in the form of depth-integrated membrane

models for both the shelf (Equation 24) and the sheet (Equations 16 and 17), with b as well as the normal components of \mathbf{U} and T_{ab} continuous at the grounding line. In one spatial dimension, the sheet model is (Muszynski & Birchfield 1987, Vieli & Payne 2005, Pattyn et al. 2006, Hindmarsh 2006a, Schoof 2007a,b)

$$\frac{\partial T_{xx}}{\partial x} - f(u)\text{sgn}(u) - \rho g b \frac{\partial s}{\partial x} = 0, \quad \frac{\partial b}{\partial t} + \frac{\partial(bu)}{\partial x} = a. \quad (28)$$

The same contact conditions as in Nowicki & Wingham (2008) now require flotation as in Equation 27 with $\tilde{k} = 1$ (Schoof 2007b, 2011). We also still have $T_{xx} = \rho(1 - \rho/\rho_w)gb^2/2$ at the grounding line.

The first term in Equation 28 is usually small except near the grounding line, and this leads to a diffusion model. With $f(u) = Cu^m$ and T_{xx} small in the interior of the ice sheet,

$$\frac{\partial s}{\partial t} + \frac{\partial q}{\partial x} = a, \quad q = \left(\frac{\rho g}{C}\right)^{1/m} (s - b)^{1+1/m} \left|\frac{\partial s}{\partial x}\right|^{-1+1/m} \frac{\partial s}{\partial x}. \quad (29)$$

Asymptotic matching with a boundary layer near the grounding line also yields a flux boundary condition (Schoof 2007b, 2011) as

$$q = \hat{k} \left[\frac{A(\rho g)^{n+1}(1 - \rho/\rho_w)^n}{4^n C} \right]^{1/(m+1)} b_g^{(m+n+3)/(m+1)} \quad (30)$$

to stand alongside the flotation condition (Equation 27). Once more \hat{k} depends only on n , m , and the density ratio (Schoof 2011). Arriving at the same result from a Stokes-flow model rather than from coupling membrane models together is considerably harder but can be done (Schoof 2011); this justifies the continuity assumptions at the grounding line made by Schoof (2007b) and also lets the model in Equation 29 be generalized to allow for vertical shear inland.

Using sophisticated numerical methods, Durand et al. (2009) extended Nowicki & Wingham's (2008) numerical solution of the Stokes-flow problem around the grounding line to cover the rapid sliding case. They found results in generally good agreement with the asymptotic theory of Schoof (2007b).

7.2. Dynamics of Marine Ice Sheets

The results above indicate the same generic structure for marine ice-sheet models in one dimension: a shallow-ice diffusion problem for the grounded sheet together with two conditions on the thickness b and flux q at the free boundaries. This leads to easily identifiable steady states: Taken together, the boundary conditions ensure that flux at the grounding line is computable as a function of grounding-line position alone. In the steady state, this flux must balance integrated mass accumulation over the ice-sheet interior.

One expects the diffusive nature of shallow-ice flow to drive marine ice sheets toward equilibrium. Weertman (1974) suggested a simple way of identifying viable equilibria: A steady state is stable only if its grounding line slopes sufficiently steeply downward so that an increase in size will cause net mass loss and hence a return to the original equilibrium. Conversely, stable grounding lines are not possible where beds slope upward; this is usually termed the marine ice-sheet instability. A mathematical demonstration of this stability property has recently been devised (Schoof 2012; see also Wilchinsky 2009 for a numerical stability analysis). An important corollary of the above is that so-called overdeepened ice-sheet beds—with a central part at a higher elevation surrounded by a deeper trough leading to a shallow part at the continental shelf edge (Figures 1 and 2)—can have multiple equilibria and experience hysteresis (Schoof 2007a), which may explain some of the observed past behavior of the West Antarctic Ice Sheet (Conway et al. 1999) and

underpins current concern that this ice sheet may undergo further irreversible shrinkage in the future. However, Weertman's argument can fail when one accounts for the isostatic depression of the underlying bedrock and the warping of sea levels caused by the ice sheet's own gravitational field (Gomez et al. 2010).

The picture becomes considerably more complicated in two dimensions. Although shelves are typically much shorter than the ice sheet, their lateral confinement in embayments (or buttressing) is highly important. With lateral shear stresses T_{xy} , the extensional stress at the grounding line is no longer a known quantity and is likely to be reduced below the one-dimensional value $\rho(1 - \rho/\rho_w)gb^2/2$. Work on this has largely been confined to numerical solutions of membrane models for the sheet and shelf (Goldberg et al. 2009, Gladstone et al. 2010); some one-dimensional models (Dupont & Alley 2005, Nick et al. 2010, Pegler & Worster 2012) have also parameterized the effect of lateral shear stresses. This has recently been put on a more consistent theoretical footing by Hindmarsh (2012). Numerical work suggests that, unlike in one dimension, solutions on upward-sloping ground can be found if the calving front is fixed (Goldberg et al. 2009), and possibly also when employing a calving model (Nick et al. 2010), or even in the absence of a shelf if the upward-sloping ground is simply confined to a narrow trough (Katz & Worster 2010). Such troughs are prevalent in many coastal areas of Antarctica and Greenland.

Calving (Winkelmann et al. 2011) and shelf-base melting by relatively warm ocean water (Holland & Jenkins 2001) become critical in two dimensions. Melting can potentially serve to steepen the shelf close to the grounding line and thereby reduce the buttressing effect of side walls. In extreme cases, melting can conceivably thin and weaken a shelf and thereby, like calving, effectively shorten the shelf (Jenkins et al. 2010) and reduce the effect of lateral drag, potentially increasing discharge through the grounding line. This remains one of the most active research areas in ice-sheet dynamics. We foresee that, in the future, complications due to the potentially localized and oscillatory nature of ice streaming described in Sections 4 and 6 will also need to be introduced to studies of marine ice sheets.

8. CONCLUSIONS

There is no single problem that acts as a limiting factor on the development of better ice-dynamics models. All the areas described above call for future improvements. However, we anticipate that successful future work will include a better understanding of thermoviscous feedbacks in ice sheets and of the bifurcation structure at the onset of oscillations and streaming behavior. Interactions between thermomechanical feedbacks, subglacial drainage, and ice-stream sliding; the patterning of ice streams; and the migration of their shear margins should be investigated. Improved constitutive relations or parameterizations of sliding and drainage are needed, constrained by more extensive field data. Finally, the dynamics of three-dimensional marine ice sheets, and their interaction with the ocean, will form a major focus for future work.

DISCLOSURE STATEMENT

The authors are not aware of any biases that might be perceived as affecting the objectivity of this review.

ACKNOWLEDGMENTS

C.G.S. acknowledges support from a Canada Research Chair and NSERC Discovery Grant number 357193. We are indebted to Evan Miles and Marianne Haseloff for extensive help with the figures and to Ed Bueler, Andrew Fowler, and Richard Hindmarsh for discussions.

LITERATURE CITED

- Alley RB. 1989. Water-pressure coupling of sliding and bed deformation: II. Velocity-depth profiles. *J. Glaciol.* 35:119–29
- Alley RB, Bindschadler RA, eds. 2001. *The West Antarctic Ice Sheet: Behavior and Environment*. Washington, DC: Am. Geophys. Union
- Alley RB, Blankenship DD, Bentley CR, Rooney ST. 1986. Deformation of till beneath ice stream B, West Antarctica. *Nature* 322:57–59
- Anandakrishnan S, Alley RB. 1997. Stagnation of Ice Stream C, West Antarctica, by water piracy. *Geophys. Res. Lett.* 24:265–68
- Aschwanden A, Blatter H. 2009. Mathematical modeling and numerical simulation of polythermal glaciers. *J. Geophys. Res.* 114:F01027
- Aschwanden A, Bueler E, Khroulev C, Blatter H. 2012. An enthalpy formulation for glaciers and ice sheets. *J. Glaciol.* 58:441–57
- Balmforth NJ, Craster RV. 2000. Dynamics of cooling domes of viscoplastic fluid. *J. Fluid Mech.* 422:225–48
- Barcilon V, MacAyeal DR. 1993. Steady flow of a viscous ice stream across a no-slip/free-slip transition at the bed. *J. Glaciol.* 39:167–85
- Bartholomew I, Nienow P, Mair D, Hubbard A, King MA, Sole A. 2010. Seasonal evolution of subglacial drainage and acceleration in a Greenland outlet glacier. *Nat. Geosci.* 3:408–11
- Benn DI, Warren CW, Mottram RH. 2007. Calving processes and the dynamics of calving glaciers. *Earth Sci. Rev.* 82:143–79
- Bindschadler RA, King MA, Alley RB, Anandakrishnan S, Padman L. 2003. Tidally controlled stick-slip discharge of a West Antarctic ice stream. *Science* 301:1087–89
- Blankenship DD, Bentley CR, Rooney ST, Alley RB. 1986. Seismic measurements reveal a saturated porous layer beneath an active Antarctic ice stream. *Nature* 322:54–57
- Blatter H. 1995. Velocity and stress fields in grounded glaciers: a simple algorithm. *J. Glaciol.* 41:333–44
- Blatter H, Greve R, Abe-Ouchi A. 2011. Present state and prospects of ice sheet and glacier modelling. *Surv. Geophys.* 32:555–83
- Bougamont M, Price S, Christoffersen P, Payne AJ. 2011. Dynamic patterns of ice stream flow in a 3D higher-order ice sheet model with plastic bed and simplified hydrology. *J. Geophys. Res.* 116:F04018
- Bougamont M, Tulaczyk S, Joughin I. 2003. Response of subglacial sediments to basal freeze-on. 2. Application in numerical modelling of the recent stoppage of Ice Stream C, West Antarctica. *J. Geophys. Res.* 108:2223
- Boulton GS, Hindmarsh RCA. 1987. Sediment deformation beneath glaciers: rheology and geological consequences. *J. Geophys. Res.* 92:9059–82
- Bueler E, Brown J. 2009. Shallow shelf approximation as a sliding law in a thermomechanically coupled ice sheet model. *J. Geophys. Res.* 114:F03008
- Bueler E, Brown J, Lingle C. 2007. Exact solutions to the thermomechanically coupled shallow-ice approximation: effective tools for verification. *J. Glaciol.* 53(182):499–516
- Calov R, Greve R, Abe-Ouchi A, Bueler E, Huybrechts P, et al. 2010. Results from the Ice-Sheet Intercomparison Project Heinrich Event Intercomparison (ISMIP HEIMO). *J. Glaciol.* 56:371–83
- Calvo N, Díaz J, Durany J, Schiavi E, Vázquez C. 2002. On a doubly nonlinear parabolic obstacle problem modelling ice sheet dynamics. *SIAM J. Appl. Math.* 63:683–707
- Catania G, Conway HB, Gades AM, Raymond C, Engelhardt H. 2003. Bed reflectivity beneath inactive ice streams in West Antarctica. *Ann. Glaciol.* 36:287–91
- Chugunov VA, Wilchinsky AV. 1996. Modelling of marine glacier and ice-sheet-ice-shelf transition zone based on asymptotic analysis. *Ann. Glaciol.* 23:59–67
- Clarke GKC. 1977. Strain heating and creep instability in glaciers and ice sheets. *Rev. Geophys.* 15:235–47
- Clarke GKC. 2005. Subglacial processes. *Annu. Rev. Earth Planet. Sci.* 33:247–76
- Conway H, Ball BL, Denton GH, Gades AM, Waddington ED. 1999. Past and future grounding-line retreat of the West Antarctic Ice Sheet. *Science* 286:280–83
- Creyts TT, Schoof CG. 2009. Drainage through subglacial water sheets. *J. Geophys. Res.* 114:F04008
- Cuffey KM, Conway H, Hallet B, Gades TM, Raymond CF. 1999. Interfacial water in polar glaciers and glacier sliding at -17°C . *Geophys. Res. Lett.* 26:751–54

- Cuffey KM, Paterson WSB. 2010. *The Physics of Glaciers*. Amsterdam: Elsevier. 4th ed.
- Das SB, Joughin I, Behn MD, Howat IM, King MA, et al. 2008. Fracture propagation to the base of the Greenland Ice Sheet during supraglacial lake drainage. *Science* 320:778–81
- Díaz JI, Muñoz AI, Schiavi E. 2007. Existence of weak solutions to a system of nonlinear partial differential equations modelling ice streams. *Nonlinear Anal. Real World Appl.* 8:267–87
- DiPietro ND, Cox R. 1979. The spreading of a very viscous liquid on a quiescent water surface. *Q. J. Mech. Appl. Math.* 32:355–81
- Dupont TK, Alley RB. 2005. Assessment of the importance of ice-shelf buttressing to ice sheet flows. *Geophys. Res. Lett.* 32:L04503
- Durand G, Gagliardini O, de Fleurian B, Zwinger T, LeMeur E. 2009. Marine ice sheet dynamics: hysteresis and neutral equilibrium. *J. Geophys. Res.* 114:F03009
- Duval P. 1977. The role of water content on the creep of polycrystalline ice. In *Isotope Impurities in Snow and Ice: Symposium at Grenoble 1975*, pp. 29–33. Int. Assoc. Hydrol. Sci. Publ. 118. Wallingford, UK: Int. Assoc. Hydrol. Sci.
- Engelhardt H, Kamb B. 1997. Basal hydraulic system of a West Antarctic ice stream: constraints from borehole observations. *J. Glaciol.* 43:207–30
- Flowers GE, Clarke GKC. 2002. A multi-component model of glacier hydrology. *J. Geophys. Res.* 107:2287
- Fountain AG, Walder JS. 1998. Water flow through temperate glaciers. *Rev. Geophys.* 36:299–328
- Fowler AC. 1981. A theoretical treatment of the sliding of glaciers in the absence of cavitation. *Philos. Trans. R. Soc. Lond. A* 298:637–85
- Fowler AC. 1984. On the transport of moisture in polythermal glaciers. *Geophys. Astrophys. Fluid Dyn.* 28:99–140
- Fowler AC. 1986a. A sliding law for glaciers of constant viscosity in the presence of subglacial cavitation. *Proc. R. Soc. Lond. A* 407:147–70
- Fowler AC. 1986b. Subtemperate basal sliding. *J. Glaciol.* 32:3–5
- Fowler AC. 1987. A theory of glacier surges. *J. Geophys. Res.* 92:9111–20
- Fowler AC. 1989. A mathematical analysis of glacier surges. *SIAM J. Appl. Math.* 49:246–63
- Fowler AC. 2001. Modelling the flow of glaciers and ice sheets. In *Continuum Mechanics and Applications in Geophysics and the Environment*, ed. B Straughan, R Greve, H Ehrentraut, Y Wang, pp. 276–304. Berlin: Springer-Verlag
- Fowler AC. 2011. *Mathematical Geoscience*. Interdiscip. Appl. Math. 36. New York: Springer-Verlag
- Fowler AC, Johnson C. 1996. Ice-sheet surging and ice-stream formation. *Ann. Glaciol.* 23:68–73
- Fowler AC, Larson DA. 1978. On the flow of polythermal glaciers. I. Model and preliminary analysis. *Proc. R. Soc. Lond. A* 363:217–42
- Fowler AC, Larson DA. 1980a. Thermal stability properties of a model of glacier flow. *Geophys. J. R. Astron. Soc.* 63:347–59
- Fowler AC, Larson DA. 1980b. The uniqueness of steady state flows in glaciers and ice sheets. *Geophys. J. R. Astron. Soc.* 63:347–59
- Fowler AC, Schiavi E. 1998. A theory of ice-sheet surges. *J. Glaciol.* 44:104–18
- Fowler AC, Toja R, Vázquez C. 2010. Temperature-dependent shear flow and the absence of thermal runaway in valley glaciers. *Proc. R. Soc. A* 466:363–82
- Frappé TP, Clarke GKC. 2007. Slow surge of Trapridge Glacier, Yukon Territory, Canada. *J. Geophys. Res.* 112:F03S32
- Gagliardini O, Cohen D, Raback P, Zwinger T. 2007. Finite-element modeling of subglacial cavities and related friction law. *J. Geophys. Res.* 112:F02027
- Gladstone RM, Lee V, Vieli A, Payne AJ. 2010. Grounding line migration in an adaptive mesh ice sheet model. *J. Geophys. Res.* 115:F04014
- Glen JW. 1958. The flow law of ice: a discussion of the assumptions made in glacier theory, their experimental foundation and consequences. In *Physics of the Movement of Ice: Symposium at Chamonix 1958*, pp. 171–83. Wallingford, UK: Int. Assoc. Hydrol. Sci.
- Glowinski R, Rappaz J. 2003. Approximation of a nonlinear elliptic problem arising in a non-Newtonian fluid flow model in glaciology. *ESAIM Math. Model. Numer. Anal.* 37:175–86

- Goldberg DN. 2011. A variationally-derived, depth-integrated approximation to a higher-order glaciological flow model. *J. Glaciol.* 57:157–70
- Goldberg D, Holland DM, Schoof C. 2009. Grounding line movement and ice shelf buttressing in marine ice sheets. *J. Geophys. Res.* 114:F04026
- Goldsby DL, Kohlstedt DL. 2001. Superplastic deformation of ice: experimental observations. *J. Geophys. Res.* 106:11017–30
- Gomez N, Mitrovica JX, Huybers P, Clark PU. 2010. Sea level as a stabilizing factor for marine-ice-sheet grounding lines. *Nat. Geosci.* 3:850–53
- Greve R. 1997. Application of a polythermal three-dimensional ice sheet model to the Greenland Ice Sheet: response to steady-state and transient climate scenarios. *J. Climate* 10:901–18
- Harrison WD, Echelmeyer KA, Larson CF. 1998. Measurement of temperature in a margin of Ice Stream B, Antarctica: implications for margin migration and lateral drag. *J. Glaciol.* 44:615–24
- Helfrich KR. 1995. Thermo-viscous fingering of flow in a thin gap: a model of magma flow in dikes and fissures. *J. Fluid Mech.* 305:219–38
- Hemming SR. 2004. Heinrich events: massive late Pleistocene detritus layers of the North Atlantic and their global imprint. *Rev. Geophys.* 42:RG1005
- Herterich K. 1987. On the flow within the transition zone between ice sheet and ice shelf. See van der Veen & Oerlemans 1987, pp. 185–202
- Hewitt IJ. 2011. Modelling distributed and channelized subglacial drainage: the spacing of channels. *J. Glaciol.* 57:302–14
- Hindmarsh RCA. 1993. Qualitative dynamics of marine ice sheets. In *Ice in the Climate System*, ed. WR Peltier, pp. 67–99. Berlin: Springer-Verlag
- Hindmarsh RCA. 2004a. A numerical comparison of approximations to the Stokes equations used in ice sheet and glacier modelling. *J. Geophys. Res.* 109:F01012
- Hindmarsh RCA. 2004b. Thermoviscous stability of ice-sheet flows. *J. Fluid Mech.* 502:17–40
- Hindmarsh RCA. 2006a. The role of membrane-like stresses in determining the stability and sensitivity of the Antarctic ice sheets: back pressure and grounding-line motion. *Philos. Trans. R. Soc. Lond. A* 364:1733–67
- Hindmarsh RCA. 2006b. Stress gradient damping of thermoviscous ice flow instabilities. *J. Geophys. Res.* 111:B12409
- Hindmarsh RCA. 2009. Consistent generation of ice-streams via thermo-viscous instabilities modulated by membrane stresses. *Geophys. Res. Lett.* 36:L06502
- Hindmarsh RCA. 2011. Ill-posedness of the shallow-ice approximation when modelling thermoviscous instabilities. *J. Glaciol.* 57:1177–78
- Hindmarsh RCA. 2012. An observationally validated theory of viscous flow dynamics at the ice shelf calving front. *J. Glaciol.* 58:375–87
- Holland DM, Jenkins A. 2001. Adaptation of an isopycnic coordinate ocean model for the study of circulation beneath ice shelves. *Mon. Weather Rev.* 129:1905–27
- Hulbe C, Fahnestock M. 2007. Century-scale discharge stagnation and reactivation of the Ross ice streams, West Antarctica. *J. Geophys. Res.* 112:F0327
- Hutter K. 1983. *Theoretical Glaciology*. Dordrecht: D. Reidel
- Iken A, Bindschadler RA. 1986. Combined measurements of subglacial water pressure and surface velocity of Findelengletscher, Switzerland: conclusions about drainage system and sliding mechanism. *J. Glaciol.* 32:101–19
- Iverson NR, Hooyer TS, Baker RW. 1998. Ring-shear studies of till deformation: Coulomb-plastic behaviour and distributed shear in glacier beds. *J. Glaciol.* 44:634–42
- Jacobson HP, Raymond CF. 1998. Thermal effects on the location of ice stream margins. *J. Geophys. Res.* 103:12111–22
- Jenkins A, Dutriew P, Jacobs SS, McPhail SD, Perrett JR, et al. 2010. Observations beneath Pine Island Glacier in West Antarctica and implications for its retreat. *Nat. Geosci.* 3:468–73
- Jouvet G, Picasso M, Rappaz J, Blatter H. 2008. A new algorithm to simulate the dynamics of a glacier: theory and applications. *J. Glaciol.* 54:801–11
- Jouvet G, Rappaz J, Bueller E, Blatter H. 2011. Existence and stability of steady-state solutions of the shallow-ice-sheet equation by an energy-minimization approach. *J. Glaciol.* 57:345–54

- Kamb B. 1970. Sliding motion of glaciers: theory and observation. *Rev. Geophys.* 8:673–728
- Kamb B. 1987. Glacier surge mechanism based on linked cavity configuration of the basal water conduit system. *J. Geophys. Res.* 92:9083–100
- Kamb B, Raymond CF, Harrison WD, Engelhardt H, Echelmeyer KA, et al. 1985. Glacier surge mechanism: 1982–1983 surge of Variegated Glacier, Alaska. *Science* 227:469–79
- Katz RF, Worster MG. 2010. Stability of ice-sheet grounding lines. *Proc. R. Soc. Lond. A* 466:1597–620
- Le Brocq A, Payne AJ, Siegert MJ, Alley RB. 2009. A subglacial water-flow model for West Antarctica. *J. Glaciol.* 55:879–88
- Lliboutry L. 1968. General theory of subglacial cavitation and sliding of temperate glaciers. *J. Glaciol.* 7:21–58
- Lliboutry L. 1987. Realistic, yet simple bottom boundary conditions for glaciers and ice sheets. *J. Geophys. Res.* 92:9101–10
- Lliboutry LA, Duval P. 1985. Various isotropic and anisotropic ices found in glaciers and polar ice caps and their corresponding rheologies. *Ann. Geophys.* 3:207–24
- Lytche MB, Vaughan DG, BEDMAP Consort. 2001. BEDMAP: a new ice thickness and subglacial topographic model of Antarctica. *J. Geophys. Res.* 106:11335–51
- MacAyeal DR. 1987. Ice-shelf backpressure: form drag versus dynamics drag. See van der Veen & Oerlemans 1987, pp. 141–60
- MacAyeal DR. 1993. Binge/purge oscillations of the Laurentide Ice Sheet as a cause of North Atlantic Heinrich events. *Paleoceanography* 8:775–84
- MacAyeal DR, Barcilon V. 1988. Ice-shelf response to ice-stream discharge fluctuations: I. Unconfined ice tongues. *J. Glaciol.* 34:121–27
- Man CS, Sun QX. 1987. On the significance of normal stress effects in the flow of glaciers. *J. Glaciol.* 33:268–73
- McTigue DF, Passman SL, Jones SJ. 1985. Normal stress effects in the creep of ice. *J. Glaciol.* 31:120–26
- Morland LW. 1987. Unconfined ice-shelf flow. See van der Veen & Oerlemans 1987, pp. 99–116
- Morland LW, Johnson IR. 1980. Steady motion of ice sheets. *J. Glaciol.* 25:229–46
- Morland LW, Shoemaker EM. 1982. Ice shelf balances. *Cold Reg. Sci. Technol.* 5:235–51
- Morland LW, Zainuddin R. 1987. Plane and radial ice-shelf flow with prescribed temperature profile. See van der Veen & Oerlemans 1987, pp. 117–40
- Muszynski I, Birchfield GE. 1987. A coupled marine ice-stream-ice-shelf model. *J. Glaciol.* 33:3–15
- Nick FM, van der Veen CJ, Vieli A, Benn DI. 2010. A physically based calving model applied to marine outlet glaciers and implications for the glacier dynamics. *J. Glaciol.* 56:781–94
- Nowicki SMJ, Wingham DJ. 2008. Conditions for a steady ice sheet–ice shelf junction. *Earth Planetary Sci. Lett.* 265:246–55
- Nye JF. 1969. A calculation of the sliding of ice over a wavy surface using a Newtonian viscous approximation. *Proc. R. Soc. Lond. A* 311:445–67
- Oerlemans J. 1981. Some basic experiments with a vertically-integrated ice sheet model. *Tellus* 33:1–11
- Pattyn F. 2003. A new three-dimensional higher-order thermomechanical ice sheet model: basic sensitivity, ice stream development, and ice flow across subglacial lakes. *J. Geophys. Res.* 108:2328
- Pattyn F, Huyghe A, De Brabander S, De Smedt B. 2006. Role of transition zones in marine ice sheet dynamics. *J. Geophys. Res.* 111:F02004
- Payne AJ, Dongelmans PW. 1997. Self-organization in the thermomechanical flow of ice sheets. *J. Geophys. Res.* 102:12219–33
- Payne A, Huybrechts P, Abe-Ouchi A, Calov R, Fastook JL, et al. 2000. Results from the EISMINT model intercomparison: the effects of thermomechanical coupling. *J. Glaciol.* 46:227–38
- Payne AJ. 1995. Limit cycles in the basal thermal regime of ice sheets. *J. Geophys. Res.* 100:4249–63
- Payne AJ, Baldwin DJ. 2000. Analysis of ice-flow instabilities identified in the EISMINT intercomparison exercise. *Ann. Glaciol.* 39:204–19
- Pegler SS, Worster MG. 2012. Dynamics of a viscous layer flowing radially over an inviscid ocean. *J. Fluid Mech.* 696:152–74
- Rappaz J, Reist A. 2005. Mathematical and numerical analysis of a three dimensional fluid flow model in glaciology. *Math. Models Methods Appl. Sci.* 15:37–52
- Raymond C. 1996. Shear margins in glaciers and ice sheets. *J. Glaciol.* 42:90–102

- Reeh N, Christensen EL, Mayer C, Olesen OB. 2003. Tidal bending of glaciers: a linear viscoelastic approach. *Ann. Glaciol.* 37:83–89
- Retzlaff R, Bentley CR. 1993. Timing of stagnation of Ice Stream C, West Antarctica, from short-pulse radar studies of buried crevasses. *J. Glaciol.* 39:553–61
- Rignot E, Kanagaratnam P. 2006. Changes in the velocity structure of the Greenland Ice Sheet. *Science* 311:986–90
- Rignot E, Mouginot J, Scheuchl B. 2011. Ice flow of the Antarctic Ice Sheet. *Science* 333:1427–30
- Robin GQ. 1955. Ice movement and temperature distribution in glaciers and ice sheets. *J. Glaciol.* 2:523–32
- Roe GH, Lindzen RS. 2001. The mutual interaction between continental-scale ice sheets and atmospheric stationary waves. *Clim. Dyn.* 17:479–87
- Röthlisberger H. 1972. Water pressure in intra- and subglacial channels. *J. Glaciol.* 11:177–203
- Saito F, Abe-Ouchi A, Blatter H. 2006. European Ice Sheet Modelling Initiative (EISMINT) model inter-comparison experiments with first-order mechanics. *J. Geophys. Res.* 111:F02012
- Sayag R, Tziperman E. 2008. Spontaneous generation of pure ice streams via flow instability: role of longitudinal shear stresses and subglacial till. *J. Geophys. Res.* 113:B05411
- Scambos TA, Bohlander JA, Shuman CA, Skvarca P. 2004. Glacier acceleration and thinning after ice shelf collapse in the Larsen B embayment. *Geophys. Res. Lett.* 31:L18402
- Schoof C. 2004. On the mechanics of ice stream shear margins. *J. Glaciol.* 50:208–18
- Schoof C. 2005. The effect of cavitation on glacier sliding. *Proc. R. Soc. Lond. A* 461:609–27
- Schoof C. 2006. A variational approach to ice-stream flow. *J. Fluid Mech.* 556:227–51
- Schoof C. 2007a. Ice sheet grounding line dynamics: steady states, stability and hysteresis. *J. Geophys. Res.* 112:F03S28
- Schoof C. 2007b. Marine ice sheet dynamics. Part I. The case of rapid sliding. *J. Fluid Mech.* 573:27–55
- Schoof C. 2010a. Coulomb friction and other sliding laws in a higher-order glacier flow model. *Math. Models Methods Appl. Sci.* 20:157–89
- Schoof C. 2010b. Ice-sheet acceleration driven by melt supply variability. *Nature* 468:803–6
- Schoof C. 2011. Marine ice sheet dynamics. Part 2. A Stokes flow contact problem. *J. Fluid Mech.* 679:122–55
- Schoof C. 2012. Marine ice sheet stability. *J. Fluid Mech.* 698:62–72
- Schoof C, Hindmarsh RCA. 2010. Thin-film flows with wall slip: an asymptotic analysis of higher order glacier flow models. *Q. J. Mech. Appl. Math.* 67:73–114
- Shumskiy PA, Krass MS. 1976. Mathematical models of ice shelves. *J. Glaciol.* 17:419–32
- Siegert MJ, Welch B, Vieli A, Blankenship DD, Joughin I, et al. 2004. Ice flow direction change in interior West Antarctica. *Science* 305:1948–51
- Solomon S, Qin D, Manning M, Marquis M, Averyt K, et al., eds. 2007. *Climate Change 2007: The Scientific Basis*. Cambridge, UK: Cambridge Univ. Press
- Sugiyama S, Gudmundsson GH. 2004. Short-term variations in glacier flow controlled by subglacial water pressure at Lauteraargletscher, Bernese Alps, Switzerland. *J. Glaciol.* 50:353–62
- Tsai VC, Rice JR. 2010. A model for turbulent hydraulic fracture and application to crack propagation at glacier beds. *J. Geophys. Res.* 115:F03007
- Tulaczyk S, Kamb WB, Engelhardt HF. 2000a. Basal mechanisms of Ice Stream B, West Antarctica: 1. Till mechanics. *J. Geophys. Res.* 105:463–81
- Tulaczyk S, Kamb WB, Engelhardt HF. 2000b. Basal mechanisms of Ice Stream B, West Antarctica: 2. Undrained plastic bed model. *J. Geophys. Res.* 105:483–94
- van den Broeke MR, Bamber J, Lennarts J, Rignot E. 2011. Ice sheets and sea level: thinking outside the box. *Surv. Geophys.* 32:495–505
- van der Veen CJ, Oerlemans J, eds. 1987. *Dynamics of the West Antarctic Ice Sheet: Proceedings of a Workshop Held in Utrecht, May 6–8, 1985*. Dordrecht: D. Reidel
- van der Veen CJ, Whillans IM. 1996. Model experiments on the evolution and stability of ice streams. *Ann. Glaciol.* 23:129–37
- van Pelt WJJ, Oerlemans J. 2012. Numerical simulations of cyclic behaviour in the Parallel Ice Sheet Model PISM. *J. Glaciol.* 58:347–60
- Vieli A, Payne AJ. 2005. Assessing the ability of numerical ice sheet models to simulate grounding line migration. *J. Geophys. Res.* 110:F01003

- Walder J. 1986. Hydraulics of subglacial cavities. *J. Glaciol.* 32:439–45
- Walder JS, Fowler AC. 1994. Channelized subglacial drainage over a deformable bed. *J. Glaciol.* 40:3–15
- Weertman J. 1957. On the sliding of glaciers. *J. Glaciol.* 3:33–38
- Weertman J. 1974. Stability of the junction of an ice sheet and an ice shelf. *J. Glaciol.* 13:3–13
- Wilchinsky AV. 2009. Linear stability analysis of an ice sheet interacting with the ocean. *J. Glaciol.* 55:13–20
- Wilchinsky AV, Chugunov VA. 2001. Modelling ice flow in various glacier zones. *J. Appl. Math. Mech.* 65:479–93
- Winkelmann R, Martin MA, Haseloff M, Albrecht T, Bueler E, et al. 2011. The Potsdam Parallel Ice Sheet Model (PISM-PIK)—Part 1: Model description. *Cryosphere* 5:715–26
- Zwally HJ, Abdalati W, Herring T, Larson K, Saba J, Steffen K. 2002. Surface-melt induced acceleration of Greenland ice-sheet flow. *Science* 5579:218–22



Contents

Hans W. Liepmann, 1914–2009 <i>Roddam Narasimha, Anatol Roshko, and Morteza Gharib</i>	1
Philip G. Saffman <i>D.I. Pullin and D.I. Meiron</i>	19
Available Potential Energy and Exergy in Stratified Fluids <i>Rémi Tailleux</i>	35
The Fluid Dynamics of Tornadoes <i>Richard Rotunno</i>	59
Nonstandard Inkjets <i>Osman A. Basaran, Haijing Gao, and Pradeep P. Bhat</i>	85
Breaking Waves in Deep and Intermediate Waters <i>Marc Perlin, Wooyoung Choi, and Zbigang Tian</i>	115
Balance and Spontaneous Wave Generation in Geophysical Flows <i>J. Vanneste</i>	147
Wave Packets and Turbulent Jet Noise <i>Peter Jordan and Tim Colonius</i>	173
Leidenfrost Dynamics <i>David Quéré</i>	197
Ice-Sheet Dynamics <i>Christian Schoof and Ian Hewitt</i>	217
Flow in Foams and Flowing Foams <i>Sylvie Cohen-Addad, Reinhard Höbner, and Olivier Pitois</i>	241
Moving Contact Lines: Scales, Regimes, and Dynamical Transitions <i>Jacco H. Snoeijer and Bruno Andreotti</i>	269
Growth of Cloud Droplets in a Turbulent Environment <i>Wojciech W. Grabowski and Lian-Ping Wang</i>	293
The Fluid Mechanics of Cancer and Its Therapy <i>Petros Koumoutsakos, Igor Pivkin, and Florian Milde</i>	325

Analysis of Fluid Flows via Spectral Properties of the Koopman Operator <i>Igor Mezić</i>	357
The Interaction of Jets with Crossflow <i>Krishnan Mabesh</i>	379
Particle Image Velocimetry for Complex and Turbulent Flows <i>Jerry Westerweel, Gerrit E. Elsinga, and Ronald J. Adrian</i>	409
Fluid Dynamics of Human Phonation and Speech <i>Rajat Mittal, Byron D. Erath, and Michael W. Plesniak</i>	437
Sand Ripples and Dunes <i>François Charru, Bruno Andreotti, and Philippe Claudin</i>	469
The Turbulent Flows of Supercritical Fluids with Heat Transfer <i>Jung Yul Yoo</i>	495

Indexes

Cumulative Index of Contributing Authors, Volumes 1–45	527
Cumulative Index of Chapter Titles, Volumes 1–45	536

Errata

An online log of corrections to *Annual Review of Fluid Mechanics* articles may be found at <http://fluid.annualreviews.org/errata.shtml>